

Gustavo G. Carrió and William R. Cotton

Department of Atmospheric Science, Colorado State University, Fort Collins, Colorado

1. INTRODUCTION

The effects of the Houston Metropolitan Area on the characteristics and intensity of convection and precipitation were investigated. We used the Regional Atmospheric Modeling System developed at Colorado State University (RAMS@CSU) coupled to the Town Energy Budget (TEB) urban model. RAMS@CSU microphysical modules consider the explicit activation of CCN (and giant CCN), a bimodal representation of cloud droplets, a bin-emulation approach for droplet collection, ice-particle riming, and sedimentation, and direct radiative effects of aerosols.

Our studies focused on events triggered by the sea-breeze circulation and were performed in two phases that used an identical modeling framework. The first phase (Carrió et al., 2010; hereafter Part I) used a case study (August 24, 2000) as a benchmark and the 1992, 2001, 2006 high-resolution National Land Cover Data (NLCD) for an objective experimental design. In addition, CCN sources of varied intensity were linked to sub-grid urban area fractions. As the relative intensification of the cells downwind of the city due to urban aerosol sources may change for environments with more or less instability we performed another series of simulations. This second phase consisted of fairly large number of multi-grid simulations (almost 100) that varied not only the intensity of the urban sources but also the value of CAPE.

In summary, our results were in agreement with previous studies, wherein enhancing CCN concentrations reduced the size of the liquid particles and increased the probability of liquid particles reaching supercooled levels as a consequence of reduced coalescence. Therefore, downwind convective cells were intensified by an additional release of latent heat as liquid particles became frozen.

However, our results also show that the effect on surface precipitation of the additional LWC carried to subzero temperature levels with increasing CCN concentrations is not monotonic. The non-monotonic behavior was linked to the riming efficiency reduction of ice particles when aerosol concentrations are further enhanced. Therefore, a greater fraction of the ice-phase condensed water mass is transported out of the storm as anvil cloud pristine ice crystals instead of being transferred to precipitating water species. Moreover, the precipitation efficiency of cells downwind of the city exhibited a similar behavior, increasing when CCN concentrations are moderately enhanced and then decreasing when aerosol concentrations are further enhanced. The pollution level for which the precipitation efficiency reaches a maximum is higher for more unstable environments.

2. MODEL CONFIGURATION

Both series of numerical experiments used the same RAMS@CSU model configuration, i.e, three two-way interactive nested grids with 42 vertical levels and horizontal grid spacing of 15, 3.75, and 0.75 km. The corresponding domain sizes were 1065 X 915km, 382.5 X 382.5km, and 151.5 X 151.5km, respectively, and the grids were centered over the city of Houston. The vertical grid was stretched with 75m spacing at the finest levels to provide better resolution within the first 1.5 km, and the model top extended to approximately 20 km above ground level.

The synoptic and mesoscale environments are simulated by grids 1 and 2, respectively, while grid 3 was used to resolve deep convection as well as the sea-breeze circulation (the location of the grids is given in Fig. 1). All simulations were heterogeneously initialized with 40 km ETA data from 24 July 2000 at 00:00 UTC and the simulation period was 24h. As done in Part I, the different grids were initialized with NLCD data allowing a much better representation of the land heterogeneities and the sub-grid area fractions of the various land-use categories considered by the model.

* *Corresponding author address:* Gustavo G. Carrió, Department of Atmospheric Science, Colorado State University, Fort Collins, CO 80526; email: carrio@atmos.colostate.edu.

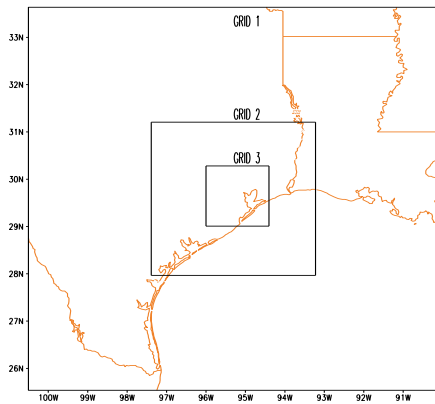


Figure 1: Grid configuration.

3. EXPERIMENTAL DESIGN

3.1 Experiments varying city size and pollution level

We considered numerical experiments using the 1992, 2001, and 2006 land-use satellite data sets as well as NO CITY run. The latter corresponds to the satellite data closest to the case used for this case study (2001), but the urban sub-grid patches were replaced by the predominant land-use categories in the city surroundings. To choose aerosol concentrations representative of a highly polluted day, we analyzed two aerosol data sets documented during TexAQS-GoMACCS: CCN measurements on the CIRPAS Twin Otter and NOAA P-3 along with other data collected by the Ronald H. Brown data for Houston and various locations of the gulf area. Peak CCN concentrations exceeded 30000 cm^{-3} , however, we eventually used lower CCN concentrations. A series of preliminary tests indicated that increasing the latter above 4000 cm^{-3} did not produce a significant impact on the results. City aerosol sources were considered by nudging these high concentrations at the first model level above the ground multiplied by the sub-grid urban fraction of the corresponding grid cell. In addition to high CCN concentrations over the city, we initialized the surroundings and the gulf area with more moderate and cleaner values, respectively. GCCN concentrations were not varied in these numerical experiments. They were initialized using O'Dowd

et al (1997) formulae for sea-salt concentrations over the gulf and lower concentrations over land. The numerical experiments corresponding to Part I are listed in Figure 2.

The city CCN concentrations represent corresponded to the maximum values (entirely urban grid cell) nudged at the first model level to consider CCN sources.

3.2 Experiments varying the strength of aerosol pollution and convective instability.

The urban CCN sources were considered by nudging different specified concentration at the first model level above the ground multiplied by the sub-grid urban fraction of the corresponding grid cell. The maximum CCN concentration we considered for an entirely urban grid cell was the same we used in Part I (the details on how this range was selected are discussed in that paper). In addition to high CCN concentrations over the city, we initialized the surroundings and the gulf area with more moderate (500 cm^{-3}) and "cleaner" (200 cm^{-3}) CCN values, respectively. All runs focused on effects of urban CCN enhancement and therefore, GCCN concentrations were homogeneously initialized in an identical manner for all runs. For that purpose, we chose the values of the sea-salt jet mode (approximately 2microns in diameter) predicted by O'Dowd et al (1997) formulae when using the wind speed over the gulf at the time of initialization.

The initial temperature field corresponding to the case study was modified to consider environments with different convective instability. We added or subtracted constant values to the temperature vertical profiles of finest grid (grid 3) approximately between cloud base and 10000 m in such a way that the convective available potential energy (CAPE) varied between 400 and 1600 Jkg^{-1} . In most cases CAPE was varied at 100 Jkg^{-1} intervals, however, we considered 50 Jkg^{-1} intervals for some urban aerosol intensities. Those temperature differences were smoothed out within grid 2 to avoid numerical discontinuities.

The list of all sensitivity experiments used in this study is given in Fig. 2. The CCN concentrations linked to the urban sources correspond to the maximum values (for entirely urban grid cell) that were used to nudge the first model level. A null intensity denotes the clean city.

This figure is also a schematic representation of how comparisons among the rather large number of multi-grid simulations are established in Section 2.3.

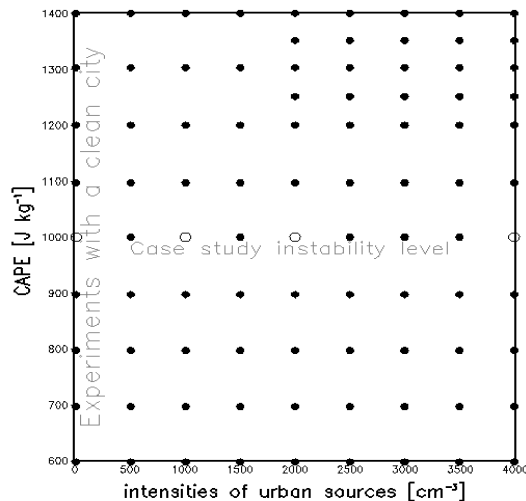


Figure 2. Numerical experiments corresponding to results presented in Section 4.2 are denoted by symbols. Open circles denote runs performed for the atmospheric conditions of the case study (Part I).

4. MAIN RESULTS

4.1 Varying city size and pollution level

In summary, when considering “larger cities”, we simulated:

- higher precipitation rates over the finest grid, the NO CITY run exhibits a maximum much later,
- the precipitation rates and accumulated values over urban cells showed lower but positive differences,
- Increased intensity of the sea breeze,
- total volume of precipitation increased monotonically 9, 11, and 30% (over NOCITY) for 1992, 2001, and 2006, respectively,

- LWPs and updrafts maxima did not change significantly, and

- conversely, the integral value of condensate and maximum downdrafts increased. The latter result is linked to the larger area coverage of the storm.

While “more polluted cities” resulted in:

- positive differences in LWC maxima for the period of intense convection,

- +4% and +9% difference for supercooled water between -10 and -20°C (~4-8km). It is well known that presence of supercooled liquid water within this temperature range plays an important role in non-inductive charge separation mechanisms, and

- a non-monotonic response of the precipitation downwind of the city when increasing CCN concentrations.

4.2 Experiments varying the strength of aerosol pollution and convective instability.

These second series of runs is not focused on the time evolution and behavior of individual storms but rather concentrated on a more macroscopic perspective of the convective cells simulated downwind of the urban complex (however, for all run the most intense convective activity downwind of the city starts between 19: and 20:00 and decays at least one hour before the end of the simulation period). This downwind region is shown in Fig 3 for the run with 2000 cm^{-3} CCN sources and 1000 Jkg^{-1} . The CCN concentrations at least twice as high as the background values (averaged over lowest 1000 m) one hour before the intense downwind convective activity develops (approximately 19:00 UTC). This region although varied when using different instability conditions did not change significantly and therefore can be considered representative of the downwind areas used to compare runs.

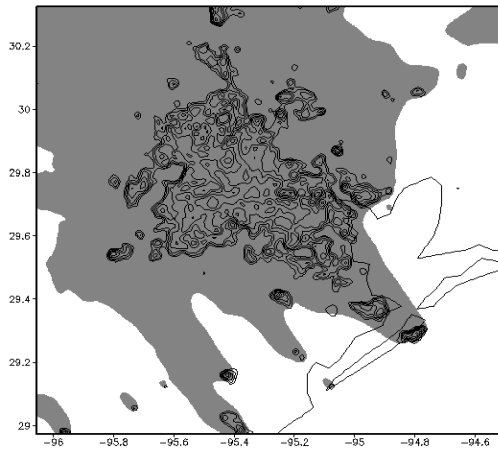


Figure 3. The shading shows the aerosol plume one hour before the convective activity in the downwind region starts (~19:00UTC).

We computed the total volume of water precipitated over the entire finest grid (grid 3) when we varied the intensity of the urban aerosol sources and CAPE values. Figure 4 shows these simulated integral volumes of precipitation relative to that of the run with the environmental conditions of case study (~1000 J kg^{-1}) and clean city. For all values of CAPE, relative differences become less important when increasing the intensity of the urban aerosol sources above 2000 cm^{-3} . This decrease is monotonic for runs with CAPE below 1000 J kg^{-1} . Conversely, the precipitated volume exhibits an initial increase for more unstable environments. It must be noted that all CAPE values, differences relative to the clean city run are very small. The simulated difference in the volumes of precipitation does not exceed 2% even when the comparison is restricted to the downwind area (not shown).

However, if we focus on the downwind precipitation accumulation in this area, relative differences can exceed 20%. Maximum accumulations within the downwind area are given in Fig. 5 for all numerical experiments in Fig. 3. Independently of the convective instability, the magnitude of this maximum first increases until it reaches a peak value and then decreases when further increasing the intensity of the aerosol sources. Higher pollution levels are required to attain the peak values (denoted by open circles) when more unstable environments are considered.

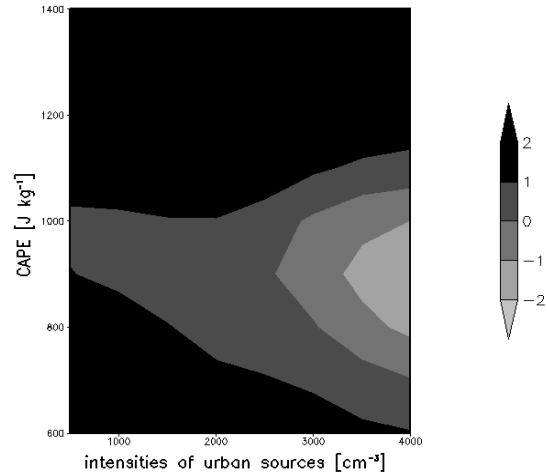


Figure 4. Comparison of the simulated integral volume of precipitation over grid 3. Shaded areas represent percent differences with respect to the run with the environmental conditions of the case study and clean city.

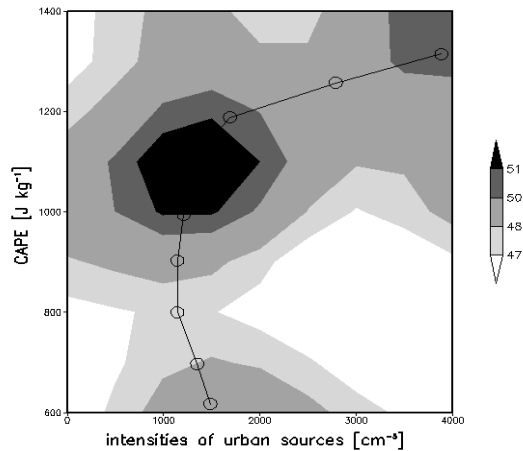


Figure 5. Comparison of the accumulated precipitation maxima [mm] over the downwind area simulated for all sensitivity runs.

Enhancing aerosol concentration tends to result in an increase of the simulated updraft maxima with respect to the value corresponding to the clean city. These differences are, in most cases, lower than 1 ms^{-1} and do not show interesting regularities when varying intensity of the urban sources (not shown). However, the altitude at which those peak updrafts are attained is

significantly affected by the urban pollution as seen in Fig. 6 that gives for each run the difference with respect to the clean city. They show a pattern similar to that of the accumulated precipitation with peak values (denoted by open triangles) requiring higher aerosol concentrations for simulations with larger CAPE values. This could be explained by the fact that the larger the overall upward flux expected higher convective instability cases would require a larger intensity of the urban sources to produce an equivalent effect.

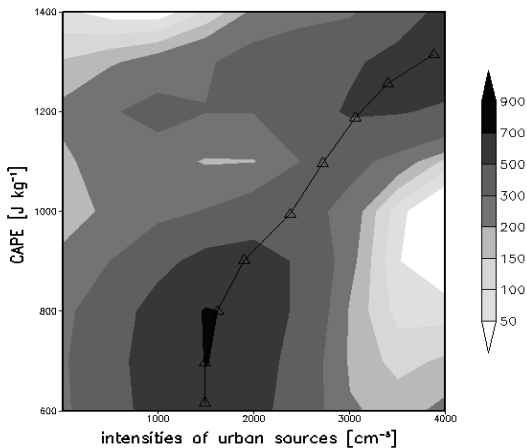


Figure 6. Comparison of the altitudes at which the maximum updraft is attained (downwind region). Shaded areas denote differences [m] with respect to the altitude that corresponds to the run with the environmental conditions of case study and a clean city. For each CAPE value, the pollution level that corresponds to the highest values is indicated by an open triangle.

For the case study, due to the increased exposure to aerosols, the upper levels of the convective cells downwind of the city were invigorated by a greater latent heat release linked to higher amounts of liquid water transported to supercooled levels. We computed the integral mass of supercooled (SC) liquid water present in the downwind area in order to compare its behavior for environments characterized by different convective instability. The corresponding peak values are given in Figure 7 for all numerical experiments in Fig. 3.

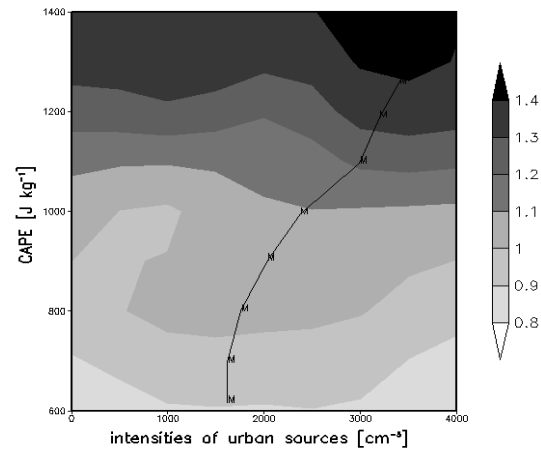


Figure 7. Maximum integral mass of SC liquid water [10^7 kg] simulated over the downwind area. The symbol *M* indicates the pollution level that corresponds to the highest value simulated for each instability environment.

Again, a similar pattern can be observed, however, the decrease for aerosol concentrations higher than the corresponding to each maximum value (denoted by an *M*) is less important for CAPE values above 1000 Jkg^{-1} . When we focused only on the layer with temperatures between -10 and -20°C (not shown), SC liquid water exhibited an almost identical response. It is well known that the presence of supercooled liquid water within this temperature range plays an important role in non-inductive charge separation mechanisms, and therefore, this result suggests an increased electrical activity within the downwind region. Figure 7 indicates that precipitation enhancement is linked to the increase of liquid mass transported to SC levels, likely to freeze and thereby release greater amounts of latent heat. However, the SC water mass remains fairly constant for runs with CAPE values above 1000 Jkg^{-1} and therefore, the decrease in the accumulations when further enhancing aerosol concentration does not appear to be related to the bulk quantity of SC liquid water mass. To explain this decrease we could either consider a decrease in the overall upward flux or a mechanism reducing the precipitation efficiency of the convective cells in the downwind area. For that reason, we computed the ratio between the

total water mass precipitated over the downwind area and the temporal integration of the upward vapor flux at approximately cloud base levels. Those ratios represent precipitation efficiencies and are given in Fig 8 for all runs. It must be noted that the peak values (denoted by an **E**) occur for higher aerosol concentrations for runs with higher CAPE and the ratios decrease when considering more intense urban aerosol sources. The latter decrease indicates that the precipitation suppression is more likely to be linked to a change in microstructure of the convective cells change than to a dynamic effect.

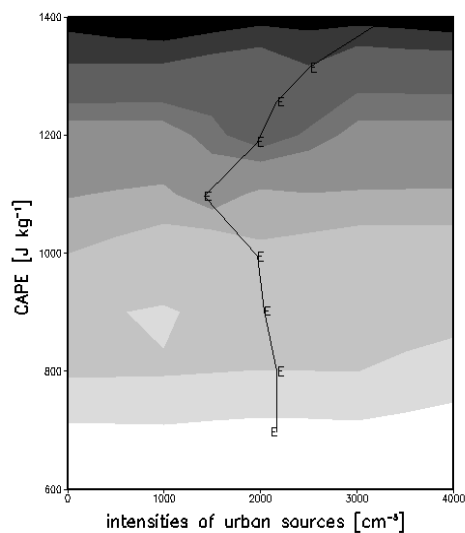


Figure 8. Precipitation efficiency estimated as the ratio [%] between the total water mass precipitated over the downwind area and the temporal integration of the upward vapor flux at approximately cloud base levels. The symbol **E indicates the pollution level that corresponds to the highest value simulated for each instability environment.**

As suggested by our results for the case study, the efficiency of the collisional mechanisms responsible for rapid freezing of SC droplets via rimming could be reduced when aerosol concentrations are further enhanced. Therefore, a greater fraction of the ice-phase condensed water mass would be transported out of the storm as

pristine ice crystals instead of being transferred to precipitating water species. To examine the role this mechanism plays when varying the convective instability, we computed a mass-weighted average of SC droplet number concentrations within the downwind area (Fig 9).

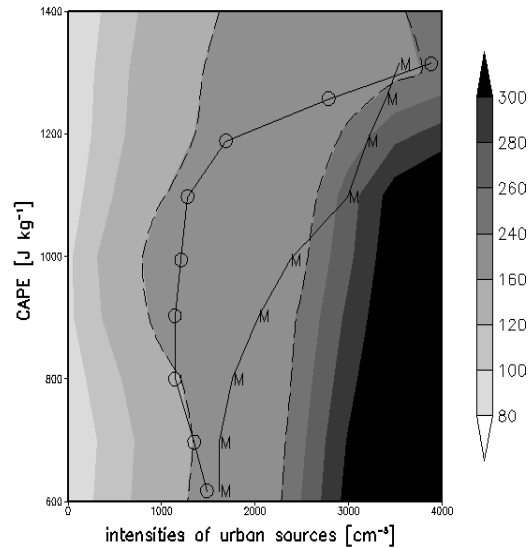


Figure 9. SC cloud droplet concentration averaged over the downwind area [cm^{-3}]. The symbol **M and the open circle indicate the pollution level that corresponds to the highest simulated values (for each instability environment) of accumulated precipitation and SC water mass, respectively.**

For each run, this averaged number concentration corresponds to the time at which the integral mass of SC liquid water reaches its maximum. The curves corresponding to the maxima of precipitation accumulation (open circles) and the integral SC water mass (symbol **M**) have been superimposed to this figure. Both curves are contained in the region where SC cloud droplet concentrations are between 140 and 240 cm^{-3} . The region corresponds to a SC droplet sizes between 4.5 to 5 microns as can be seen in Fig 10 that is analogous to Fig. 9 but gives SC droplet diameters.

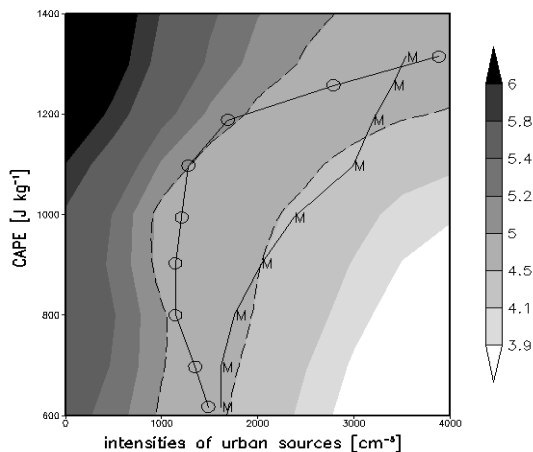


Figure 12. Analogous to Fig. 10 but for the SC cloud droplet diameter [microns]. Shaded areas correspond to mass-weighted diameters.

5. CONCLUSIONS

Results indicate that particulate pollution can significantly intensify convective cells occurring downwind of an urban complex. The simulated precipitation accumulations can increase up to 12% within this region however, the integral effect on the precipitation volumes is less important. For instance, differences were in all cases lower than 2% the entire finest grid was considered. It must be noted that our results show a non monotonic response of precipitation in the downwind region when more polluted cities were considered, independently of the value of CAPE. This type of behavior was also observed in Part I when we considered different city sizes for the atmospheric conditions of August 24 2000. It first increases from the clean city run to a certain level of particulate pollution and then decreases when considering more intense urban sources. This initial increase, in agreement with several previous studies, is linked to greater amounts of liquid water being thrust aloft in supercooled levels that eventually freezes releasing greater amounts of latent heat of freezing. Basically, this greater availability of SC liquid water is associated with a lower efficiency of the warm rain process. However, further enhancing cloud-nucleating aerosol concentrations starts reducing the

efficiencies of the mechanisms involving SC droplets and pristine ice crystals (as well as other ice phase hydrometers). The riming growth of ice particles is responsible of the rapid transfer of this SC liquid water to the ice phase, and therefore the reduction of its efficiency increases the fraction of the ice-phase condensed water mass is transported out of the storm as pristine ice crystals instead of being transferred to precipitating water species, explaining the non-monotonic response. Simulated maxima of updrafts, integral mass of SC liquid water, and precipitation efficiency also exhibited a response similar to that of the maximum accumulated precipitation. Even when increasing the pollution levels did not have a significant impact on the simulated peak updrafts, the maxima occurred at altitudes higher than that of the clean city for all urban source intensities. When considering more polluted cities, these altitude differences as well as the amounts of SC liquid water and precipitation efficiency first increase and then decrease. However, the aforementioned change of response to the enhancement of CCN concentration is more evident when comparing the mass-weighted size (and number concentrations) of SC liquid droplets; the precipitation efficiency starts to decrease when SC liquid droplet diameter is lower than approximately 4.5-5 microns.

On the other hand, the peak values of all simulated quantities were simulated for more intense urban CCN sources when more unstable environments were considered. This can be easily explained as higher convective instability levels generates larger the overall upward fluxes and therefore more intense CCN sources would be required to produce an equivalent microphysical effect. The expected increase of the particulate pollution is more likely to selective enhance precipitation and electrical activity of convective events characterized by higher instability.

Finally, our results indicate no significant impact of *direct* radiative effect for these sea-breeze induced summer storms.

6. ACKNOWLEDGEMENTS

Gustavo Carrió, and William Cotton were funded by NOAA grant #NA070AR4310281 (CSU #5-31231).

7. REFERENCES

Carrió, G. G., Cotton, W. R., Cheng W. Y. Y., 2010: Urban growth and aerosol effects on convection over Houston. Part I: the August 2000 case. *Atmos. Res.*, 96, 560-574.

Dowd, C.D., M.E. Smith, I.E. Consterdine and J.A. Lowe, 1997: Marine aerosol, sea-salt, and the marine sulphur cycle: A short review. *Atmos. Environ.*, 31, 73-80.